Brain Advance Access published April 17, 2016

doi:10.1093/brain/aww079 BRAIN 2016: Page 1 of 16 | 1

BRAIN
A JOURNAL OF NEUROLOGY

SYNE1 ataxia is a common recessive ataxia with major non-cerebellar features: a large scale multi-centre study

Matthis Synofzik,[1,2,*] Katrien Smets,[3,4,5,*] Martial Mallaret,[6,7,*] Daniela Di Bella,[8,*] Constanze Gallenmüller,[9,10,11] Jonathan Baets,[3,4,5] Martin Schulze,[12] Stefania Magri,[8] Elisa Sarto,[8] Mona Mustafa,[13] Tine Deconinck,[3,5] Tobias Haack,[14,15] Stephan Züchner,[16] Michael Gonzalez,[16] Dagmar Timmann,[17] Claudia Stendel,[9,10] Thomas Klopstock,[9,10,11] Alexandra Durr,[18] Christine Tranchant,[6,7] Marc Sturm,[12] Wahiba Hamza,[19] Lorenzo Nanetti,[8] Caterina Mariotti,[8] Michel Koenig,[7,20] Ludger Schöls,[1,2] Rebecca Schüle,[1,2,16] Peter de Jonghe,[3,4,5,#] Mathieu Anheim,[6,7,21,#] Franco Taroni[8,#] and Peter Bauer[12,#]

[*,#]These authors contributed equally to this work.

Mutations in the synaptic nuclear envelope protein 1 (*SYNE1*) gene have been reported to cause a relatively pure, slowly progressive cerebellar recessive ataxia mostly identified in Quebec, Canada. Combining next-generation sequencing techniques and deep-phenotyping (clinics, magnetic resonance imaging, positron emission tomography, muscle histology), we here established the frequency, phenotypic spectrum and genetic spectrum of *SYNE1* in a screening of 434 non-Canadian index patients from seven centres across Europe. Patients were screened by whole-exome sequencing or targeted panel sequencing, yielding 23 unrelated families with recessive truncating *SYNE1* mutations (23/434 = 5.3%). In these families, 35 different mutations were identified, 34 of them not previously linked to human disease. While only 5/26 patients (19%) showed the classical *SYNE1* phenotype of mildly progressive pure cerebellar ataxia, 21/26 (81%) exhibited additional complicating features, including motor neuron features in 15/26 (58%). In three patients, respiratory dysfunction was part of an early-onset multisystemic neuromuscular phenotype with mental retardation, leading to premature death at age 36 years in one of them. Positron emission tomography imaging confirmed hypometabolism in extra-cerebellar regions such as the brainstem. Muscle biopsy reliably showed severely reduced or absent SYNE1 staining, indicating its potential use as a non-genetic indicator for underlying *SYNE1* mutations. Our findings, which present the largest systematic series of SYNE1 patients and mutations outside Canada, revise the view that SYNE1 ataxia causes mainly a relatively pure cerebellar recessive ataxia and that it is largely limited to Quebec. Instead, complex phenotypes with a wide range of extra-cerebellar neurological and non-neurological dysfunctions are frequent, including in particular motor neuron and brainstem dysfunction. The disease course in this multisystemic neurodegenerative disease can be fatal, including premature death due to respiratory dysfunction. With a relative frequency of ~5%, SYNE1 is one of the more common recessive ataxias worldwide.

1 Department of Neurodegenerative Diseases, Hertie-Institute for Clinical Brain Research, University of Tübingen, Germany
2 German Research Center for Neurodegenerative Diseases (DZNE), University of Tübingen, Germany
3 Neurogenetics Group, VIB-Department of Molecular Genetics, University of Antwerp, BelgiumVIB-Department of Molecular Genetics, University of Antwerp, Belgium
4 Department of Neurology, Antwerp University Hospital, Belgium
5 Laborator Laboratory of Neurogenetics, Institute Born-Bunge, University of Antwerp, Belgium

Received September 12, 2015. Revised December 09, 2015. Accepted January 11, 2016.

6 Department of Neurology, Hôpital de Hautepierre, Strasbourg, France
7 Institut de Génétique et de Biologie Moléculaire et Cellulaire (IGBMC), INSERM-U964/CNRS-UMR7104/Université de Strasbourg, Collège de France, 67404 Illkirch, France
8 Unit of Genetics of Neurodegenerative and Metabolic Diseases, Fondazione IRCCS Istituto Neurologico Carlo Besta, Milan, Italy
9 Department of Neurology with Friedrich-Baur-Institute, Ludwig-Maximilians-University, Munich, Germany
10 German Research Center for Neurodegenerative Diseases (DZNE), Munich, Germany
11 Munich Cluster for Systems Neurology (SyNergy), Munich, Germany
12 Institute of Medical Genetics and Applied Genomics, University of Tübingen, Germany
13 Department of Nuclear Medicine, Ludwig-Maximilians-University, Munich, Germany
14 Institute of Human Genetics, Technische Universität München, 81675 Munich, Germany
15 Institute of Human Genetics, Helmholtz Zentrum München, German Research Center for Environmental Health, 85764 Neuherberg, Germany
16 Dr. John T. Macdonald Foundation Department of Human Genetics and John P. Hussman Institute for Human Genomics, University of Miami Miller School of Medicine, Miami, USA
17 Department of Neurology, University of Duisburg-Essen, Essen, Germany
18 APHP Genetic department and Centre de Recherche de l'Institut du Cerveau et de la Moelle épinière (ICM), UPMC University Paris VI, UMR975; CNRS UMR 7225; INSERM U975; University Hospital Pitié-Salpêtrière, 75013 Paris, France
19 Laboratoire de Biologie Cellulaire et Moléculaire, Faculté des Sciences Biologiques, USTHB, Algiers, Algeria
20 Laboratoire de Genetique de Maladies Rares, EA 7402, Institut Universitaire de Recherche Clinique, Université et CHU de Montpellier, 34093 Montpellier cedex 5, France
21 Fédération de Médecine Translationnelle de Strasbourg (FMTS), Université de Strasbourg, Strasbourg, France

Correspondence to: Dr Matthis Synofzik,
Department of Neurodegenerative Diseases,
University of Tübingen,
Hoppe-Seyler-Str. 3, 72076 Tübingen,
Germany
E-mail: matthis.synofzik@uni-tuebingen.de

Keywords: ataxia; motor neuron disease; hereditary spastic paraplegia; genetics; Nesprin 1

Abbreviations: ARCA = autosomal recessive cerebellar ataxia; EDMD4 = Emery-Dreifuss muscular dystrophy type 4; FDG = fluorodeoxyglucose

Introduction

SYNE1 (OMIM 608441) is one of the largest genes in the human genome, with the longest isoform comprising 146 exons that encode the 8797 amino-acid synaptic nuclear envelope protein 1 (Gros-Louis *et al.*, 2007). This protein, also known as Nesprin 1 (Nuclear envelope spectrin 1), is part of the spectrin family of structural proteins that share a common function of linking the plasma membrane to the actin cytoskeleton (Gros-Louis *et al.*, 2007). Truncating recessive mutations in *SYNE1* have been reported to cause a slowly progressive, relatively pure cerebellar ataxia with only few extra-cerebellar symptoms (spinocerebellar ataxia, autosomal-recessive 8; SCAR8/autosomal-recessive cerebellar ataxia type 1, ARCA1) (Dupre *et al.*, 1993/2012, 2007; Gros-Louis *et al.*, 2007; Noreau *et al.*, 2013; Fogel *et al.*, 2014). So far, this ataxia has been mainly observed in Quebec, Canada: while it presents the third most common hereditary ataxia in Quebec [after ARSACS (autosomal recessive spastic ataxia of Charlevoix-Saguenay) and Friedreich ataxia] (Dupre *et al.*, 1993/2012, Gros-Louis *et al.*, 2007), only few families have been identified outside French-Canadian populations so far (Izumi *et al.*, 2013; Noreau *et al.*, 2013; Hamza *et al.*, 2015). This view on the phenotype and geographic distribution of *SYNE1* ataxia, however, might be rather preliminary, given that systematic screenings outside this founder population were confined to highly selected individual cases (Izumi *et al.*, 2013; Noreau *et al.*, 2013). A systematic characterization of the clinico-genetic spectrum of a larger non-French-Canadian subject group is missing. We here hypothesized that (i) *SYNE1* is a frequent cause of recessive ataxia also outside French-Canadian populations, given the large size of the *SYNE1* gene; and (ii) dysfunction in extra-cerebellar systems is not the exception but the rule. To test these hypotheses, we aggregated the genetic and phenotypic findings of a screening of 434 ataxia patients compiled by seven different European centres, unravelling 23 novel index patients with truncating *SYNE1* mutations, including 34 mutations not previously linked to human disease. This large collection of *SYNE1* patients demonstrates that *SYNE1* ataxia is a common recessive ataxia also outside the French-Canadian founder population, and that it commonly presents with multisystemic neurodegenerative disease. This includes in particular motor neuron and brainstem features and even complex neuromuscular

syndromes, where respiratory dysfunction can lead to premature death.

Materials and methods

Patients

Four hundred and thirty-four index subjects with unexplained early-onset degenerative ataxia (age of onset < 40 years) compatible with autosomal recessive inheritance (no ataxia in the parental generation) and negative for trinucleotide repeat expansions causing Friedreich's ataxia (FRDA) were compiled from seven different European ataxia centres ($n = 116$ Tübingen, Germany; $n = 16$ Essen, Germany; $n = 13$ Munich, Germany; $n = 109$ Milano, Italy; $n = 139$ Strasbourg and Paris, France; $n = 41$, Antwerp, Belgium). These patients originated from 36 different countries (Supplementary material).

Genetic screening using next-generation sequencing

Subjects were screened for *SYNE1* mutations by one of the following five next-generation sequencing methods: (i) as part of a high coverage HaloPlex gene panel kit (Agilent), which included > 120 known ataxia genes ($n = 179$); (ii) as part of a targeted exon-capture sequencing strategy (Agilent SureSelect kit), which included 57 known ataxia genes ($n = 139$); (iii) as part of an amplicon-based customized panel (Illumina TrueSeq Custom Amplicon, TSCA) covering 76 known ataxia genes ($n = 21$); (iv) as part of a targeted exon-capture sequencing strategy (Illumina Nextera Rapid Capture Custom kit), which included 107 known ataxia genes ($n = 54$); or (v) as part of whole-exome sequencing using the SureSelect Human All Exon 50Mb kit (Agilent) ($n = 41$). Further details of these five methods can be found in the Supplementary material.

Variants were filtered for (i) non-synonymous homozygous or compound heterozygous truncating mutations in *SYNE1* (frameshift insertions or deletions, splice mutations, and stop-gain mutations); that were (ii) absent or extremely rare (minor allele frequency < 0.5%) in the public databases GEM.app (5992 exomes from 4279 families) (Gonzalez *et al.*, 2013, 2015), dbSNP137, NHLBI ESP6500, 1000Genomes project, and ExAc (60706 exomes; Exome Aggregation Consortium; http://exac.broadinstitute.org, accessed 06/2015) (for further details on the next-generation sequencing bioinformatics and filter criteria, see Supplementary material). Ninety to ninety-five per cent of the coding exons of *SYNE1* have been covered with > 20 reads by all five test formats.

In addition, to screen for *SYNE1* exon deletions/duplications, we performed a preliminary copy number variation analysis on our panel–sequencing datasets from 229 patients of the ataxia screening cohort (Supplementary material).

Inclusion of *SYNE1* missense variants

Due to the high number of private missense variants in the large *SYNE1* gene (often located in the numerous, modestly conserved spectrin repeats of the gene) and given the fact that only truncating *SYNE1* variants have been established as a cause of *SYNE1* ataxia, we did not include cases carrying only *SYNE1* missense variants. Following a conservative approach towards SYNE1 missense variants, subjects carrying a missense variant were only included if the respective missense variant (i) segregated *in trans* with a truncating *SYNE1* variant; (ii) was absent or rare in public exome databases (same criteria as above); (iii) located in highly conserved positions of the N-terminal actin-binding domain (codon 1–289); and (iv) predicted to be damaging by at least two out of three *in silico* algorithms [Mutation Taster (Schwarz *et al.*, 2010; Wang *et al.*, 2010); SIFT (Sim *et al.*, 2012); and PolyPhen-2 (Adzhubei *et al.*, 2010)]. These criteria lead to the inclusion of one *SYNE1* missense mutation (p.F220S) in the final cohort. The mutation p.D5140G (Family 7), which presented as a missense mutation on the genomic level, was shown to result in aberrant splicing of *SYNE1* transcript, thus representing *de facto* a null mutation.

Burden analysis of *SYNE1* missense variants

To further explore the significance of SYNE1 missense variants in ataxia, we tested whether rare missense SYNE1 variants predicted to be damaging were more frequent in cases with ataxia than in controls. Cases comprised of a consecutive series of $n = 96$ whole exome datasets from index patients with early-onset ataxia (same inclusion criteria as above). Controls comprised of a consecutive series of $n = 250$ whole exome datasets from index subjects with early-onset Alzheimer's disease, a condition that is not part of the extended phenotypic spectrum of SYNE1 demonstrated here (Supplementary material).

Messenger RNA analysis

Messenger RNA analysis was performed for selected mutations (mutations of Families 6 and 7) to confirm the effect of the cryptic splice mutation identified in this study (Family 7), and to exemplarily confirm the loss-of-function mechanism of truncating *SYNE1* mutations through nonsense-mediated decay of mutant mRNA (Family 6). Total RNA was extracted from lymphocytes using a Maxwell® Extractor (Promega) with the Maxwell® 16 LEV simply RNA Cells kit. Complementary DNA synthesis was carried out using Transcriptor FirstStrand cDNA synthesis kit (Roche) with random primers. PCR was carried out in 20 µl with an annealing temperature of 58 °C and specific primer pairs designed to amplify cDNA fragments encompassing the different mutations of Families 6 and 7. The amplified fragments were directly sequenced on an automated sequencer (ABI Prism 3100 Genetic Analyzer, Applied Biosystems) using the BigDye® Deoxy Terminator Cycle Sequencing Kit (Applied Biosystems) according to the manufacturer's recommendations.

Histological analysis and immunohistochemistry of muscle tissue

Biopsies of the quadriceps muscle were available from three *SYNE1* subjects and compared to a healthy age-matched control. The samples were analysed by classical histological, histochemical, histoenzymatic and immunohistochemical

techniques, as described previously (Martin *et al.*, 1997). The antibodies used were mouse monoclonal anti-emerin (NCL-emerin, 1/100, acetone fixation, Novocastra); mouse monoclonal anti-lamin A/C (NCL-LAM-A/C, 1/1000, aceton/methanol fixation, Novocastra) and rabbit polyclonal anti-nesprin-1 (PRB-439P, 1/2000, unfixated, Covance). The avidin-biotin complex technique for the monoclonal antibodies and the peroxidase-antiperoxidase technique were used for the polyclonal antibody.

Clinical and electrophysiological assessments

All index patients carrying two pathogenic *SYNE1* alleles (either in homozygous or compound heterozygous state) as well as their affected siblings received a systematic clinical assessment for disturbances in multiple neurological systems (Table 2) by a movement disorder specialist. Nerve conduction studies and EMG investigations were performed in all patients available for these investigations. Patients were classified into two phenotypic categories: (i) pure cerebellar ataxia (only ataxia features without any evidence of non-ataxia features); or (ii) cerebellar ataxia plus (ataxia plus clinical evidence for damage of at least one additional neurological system, such as e.g. upper and/or lower motor neuron disease). Disease severity was rated by the Scale for the Assessment and Rating of Ataxia (SARA) (Schmitz-Hubsch *et al.*, 2006).

MRI and PET imaging

Routine brain MRI including T_1-, T_2-, diffusion-weighted images and fluid attenuated inversion recovery T_2 (FLAIR) images were performed for at least one patient per family and were reviewed by both neuroradiologists and a neurologist. ^{18}F-fluorodeoxyglucose (FDG)-PET imaging was performed for two exemplary subjects with ataxia-motor neuron disease on a Siemens ECAT HR + scanner (CTI) with a 128 × 128 voxel matrix (voxel size 2 mm), an axial field of view of 15.5 mm and a full-width at half-maximal resolution of 5 mm, according to previously published tracer-specific protocols (Forster *et al.*, 2010). Resting-state PET recordings were obtained in the interval 30–50 min after intravenous application of 200 MBq 18-Fluoro-2-deoxyglucose (^{18}F-FDG) in fasting state (> 6 h), a brief attenuation scan was obtained with integrated ^{68}Ge rod sources (for details of image analysis, see Supplementary material).

Results

A large cohort of novel *SYNE1* index families and mutations from European and non-European populations

We identified 22 index patients carrying two truncating *SYNE1* alleles and one index patient carrying one truncating plus one missense *SYNE1* allele, thus yielding a total of 23 index patients out of 434 early-onset ataxia patients (5.3%). Five index patients were from multiplex families, the remaining 18 index patients were simplex cases. Six index patients had consanguineous parents. In the 23 index patients, we observed a total of 35 different mutations, consisting of seven frameshift, 20 nonsense mutations, six nucleotide changes affecting constitutive splice sites, one nucleotide change generating a cryptic exonic splice site, and one missense mutation in the actin binding domain (Table 1; for a discussion of the cryptic exonic splice site and the missense mutation, see below). The mutations were spread across the giant *SYNE1* gene, including the acting binding domain (also called calponin homology domain containing actin binding site) and the spectrin repeat domains (Fig. 1A). Five mutations (mutations 1–5) also affect the coding sequence of the SYNE1 isoform Nesprin 1α (nucleotide reference: http://www.ncbi.nlm.nih.gov/nucleotide/119120815), a region where no mutations linked to ataxia have been previously found (Razafsky and Hodzic, 2015). Thirty-four of thirty-five mutations have not reported in association with human disease before, thus more than doubling the total amount of all *SYNE1* truncating mutations that have been published so far (for overview of all novel and published mutations, see Fig. 1B). Only the variant c.3736G > T, p.E1246* (mutation 29, Table 1) has been reported before (Hamza *et al.*, 2015). Two mutations were listed in dbSNP/1000 Genomes database, but also not yet linked with human disease. All 35 mutations were absent or had extremely low minor allele frequency (< 0.001%) in GEM.app (5992 exomes from 4279 families), dbSNP137, 1000 Genomes database, NHLBI ESP (6500 exomes), ExAc (60706 exomes) (Table 1). Moreover, all 35 mutations yielded a scaled CADD score (combined annotation dependent depletion) of ⩾ 19 (Table 1), ranking the predicted pathogenicity of each mutation among the top 1% of all 8.6 billion single nucleotide variants in the GRCh37/hg19 (Kircher *et al.*, 2014). All mutations were confirmed by Sanger sequencing. In all families where DNA from the siblings was available (10/23), the variants co-segregated with disease in affected siblings, and unaffected siblings carried at most one pathogenic allele. For all families where DNA of at least one parent was available (12/23 families), we were able to show that the respective parent carried only one of the respective two *SYNE1* variants, indicating a biallelic localization of the variants in the index child. In four of the remaining 11 families, consanguinity was also suggestive of a biallelic location of the observed homozygous mutations. No other significant variants in known ataxia genes were identified in any of the 23 index subjects, as demonstrated by screening through whole exome sequencing and targeted panel sequencing, respectively.

No obvious *SYNE1* multi-exon deletions/duplications were observed by our preliminary next generation sequencing-based copy number variation analysis (Supplementary material). This result, however, has to be interpreted with caution as no consensus currently exists on a method to perform copy number variation analysis on next generation sequencing data.

Table 1 SYNE1 mutations identified in this study

Variant ID	Family ID	Phenotype	Genomic variant	cDNA variant	Protein change	Variant type	Zygosity	PhyloP	CADD score	MAF 1000 Genomes | rs# dbsnp	MAF ExAC	MAF EVS6500	In HGMD
1	#8	CA plus	chr6:152456368C>T	c.25516-1G>A	-NA-	Splicing	Het	7.62	29.1	0	0	0	Absent
2	#18	pCA	chr6:152473139C>T	c.24054G>A	p.W8018*	Stopgain SNV	Het	7.625	61	0	0	0	Absent
3	#4	CA plus	chr6:152473168G>A	c.24025C>T	p.Q8009*	Stopgain SNV	Het	5.634	60	0	0	0	Absent
4	#5, #23	CA plus	chr6:152476161G>A	c.23782C>T	p.R7928*	Stopgain SNV	Het	1.316	59	0 |rs570916267	0	0	Absent
5	#7	pCA	chr6:152477125insCACTCGGCATCAGTGGCACAGGCGT	c.23684_23685insACGCCTGTGCCACTGATGCCGAGTG	p.C7895*	Frameshift duplication | stopgain	Het	-NA-	54	0	0	0	Absent
6	#12	CA plus	chr6:152542097G>T	c.21528C>A	p.Y7176*	Stopgain SNV	Het	0.153	58	0	0	0	Absent
7	#9	CA plus	chr6:152542688G>A	c.21316C>T	p.Q7106*	Stopgain SNV	Het	9.038	60	0	0	0	Absent
8	#12	CA plus	chr6:152551729G>A	c.20935C>T	p.R6979*	Stopgain SNV	Het	1.371	41	0	0	0	Absent
9	#14	CA plus	chr6:152555035G>A	c.20380C>T	p.Q6794*	Stopgain SNV	Het	9.476	60	0	0	0	Absent
10	#23	CA plus	chr6:152557241C>G	c.G20183 + 1G>C	-NA-	Splicing	Het	7.808	33	0	0	0	Absent
11	#11	CA plus	chr6:152558041G>A	c.19897C>T	p.Q6633*	Stopgain SNV	Homo	7.646	59	0	0	0	Absent
12	#10	CA plus	chr6:152558084C>G	c.19855-1G>C	-NA-	Splicing	Homo	7.304	28.1	0	0	0	Absent
13	#19	CA plus	chr6:152605163G>A	c.17944C>T	p.R5982*	Stopgain SNV	Homo	1.582	50	0	0	0	Absent
14	#14	CA plus	chr6:152615251insT	c.17480dup	p.Y5827*	Frameshift insertion| stopgain	Het	-NA-	38	0	0	0	Absent
15	#18	pCA	chr6:152639275-152639281 delTCAGTTT	c.16294_16300delAAACTGA	p.K5432Lfs*25	Frameshift deletion	Het	-NA-	40	0	0	0	Absent
16	#3	pCA	chr6:152642966G>A	c.15760C>T	p.R5254*	Stopgain SNV	Homo	5.373	53	0	0	0	Absent
17	#4	CA plus	chr6:152644651-152644652delGA	c.15665_15666delTC	p.L5222Hfs*21	Frameshift deletion	Het	-NA-	35	0	0	0	Absent
18	#7	pCA	chr6:152646244T>C	c.15419A>G	p.D5140Gfs1*	(Cryptic) splicing	Het	3.931	19.05	0	8.2×10^{-6}	0	Absent
19	#2	CA plus	chr6:152651038G>A	c.14569C>T	p.Q4857*	Stopgain SNV	Het	7.928	51	0	0	0	Absent
20	#21	CA plus	chr6:152651345insA	c.14261dup	p.Q4755Profs*15	Frameshift insertion	Het	-NA-	36	0	0	0	Absent
21	#6	CA plus	chr6:152651352-152651352delC	c.14255delG	p.G4752Efs*10	Frameshift deletion	Het	-NA-	36	0	0	0	Absent
22	#1	pCA	chr6:152652521-152652521delG	c.13086delC	p.H4362Qfs*2	Frameshift deletion	Homo	-NA-	24.8	0	0	0	Absent
23	#15	CA plus	chr6:152657975C>T	c.12315 + 1G>A	-NA-	Splicing	Homo	7.499	26.2	0	0	0	Absent
24	#9	CA plus	chr6:152665320G>A	c.11908C>T	p.R3970*	Stopgain SNV	Het	6.313	51	0	0	0	Absent
25	#5	CA plus	chr6:152706854insAT	c.8627_8628insAT	p.M2876Ifs*19	Frameshift insertion	Het	-NA-	34	0	0	0	Absent
26	#8	CA plus	chr6:152711589T>C	c.8026-2A>G	-NA-	Splicing	Het	7.542	25.6	0	0	0	Absent
27	#16	pCA	chr6:152722345C>T	c.6978G>A	p.W2326*	Stopgain SNV	Homo	5.118	20.3	0	0	0	Absent
28	#21	CA plus	chr6:152737559G>A	c.6034C>T	p.R2012*	Stopgain SNV	Het	0.595	32	0,0002 | rs200119679	8.2×10^{-6}	0	Absent
29	#17	CA plus	chr6:152765668C>A	c.3736G>T	p.E1246*	Stopgain SNV	Homo	5.495	39	0	0	0	Absent
30	#20	CA plus	chr6:152776698T>A	c.2776A>T	p.K926*	Stopgain SNV	Het	3.905	36	0	0	0	Absent
31	#22	CA plus	chr6:152826408G>A	c.727C>T	p.R243*	Stopgain SNV	Homo	0.771	35	0	0	0	Absent
32	#13	CA plus	chr6:152826453G>A	c.682C>T	p.R228*	Stopgain SNV	Homo	4.534	36	0	8.2×10^{-6}	0	Absent
33	#20	CA plus	chr6:152826476A>G	c.659T>C	p.F220S	Missense	Het	9.339	28.8	0	0	0	Absent
34	#6	CA plus	chr6:152832174A>T	c.395T>A	p.L132*	Stopgain SNV	Het	9.14	38	0	1.6×10^{-5}	0	Absent
35	#2	CA plus	chr6:152841593C>T	c.309 + 1G>A	-NA-	Splicing	Het	7.187	27.8	0	0	0	Absent

Genomic positions of the variants according to genome build hg19. DNA changes according to NM_033071.3. Variant type and protein changes according to GVS function based on NP_149062. pCA = pure cerebellar ataxia; CA plus = cerebellar ataxia plus clinical evidence for damage of at least one additional neurological system; PhyloP = PhyloP conservation score based on base-wise conservation across 100 vertebrates; CADD score = scaled Combined Annotation Dependent Depletion score, integrating many diverse annotations into a single measure (C score) for each variant. The predicted pathogenicity of each variant is scored and ranked relative to all ~8.6 billion single nucleotide variants of the GRCh37/hg19 reference. A scaled CADD score of 20 indicates variants at the top 1%, a CADD score of 30 indicates variants at the top 0.1%, etc. (Kircher *et al.*, 2014). MAF = minor allele frequency; ExAC = Exome Aggregation Consortium; EVS = Exome Variant Server 6500 exomes all from the NHLBI GO Exome Sequencing Project; HGMD = Human Gene Mutation Database.

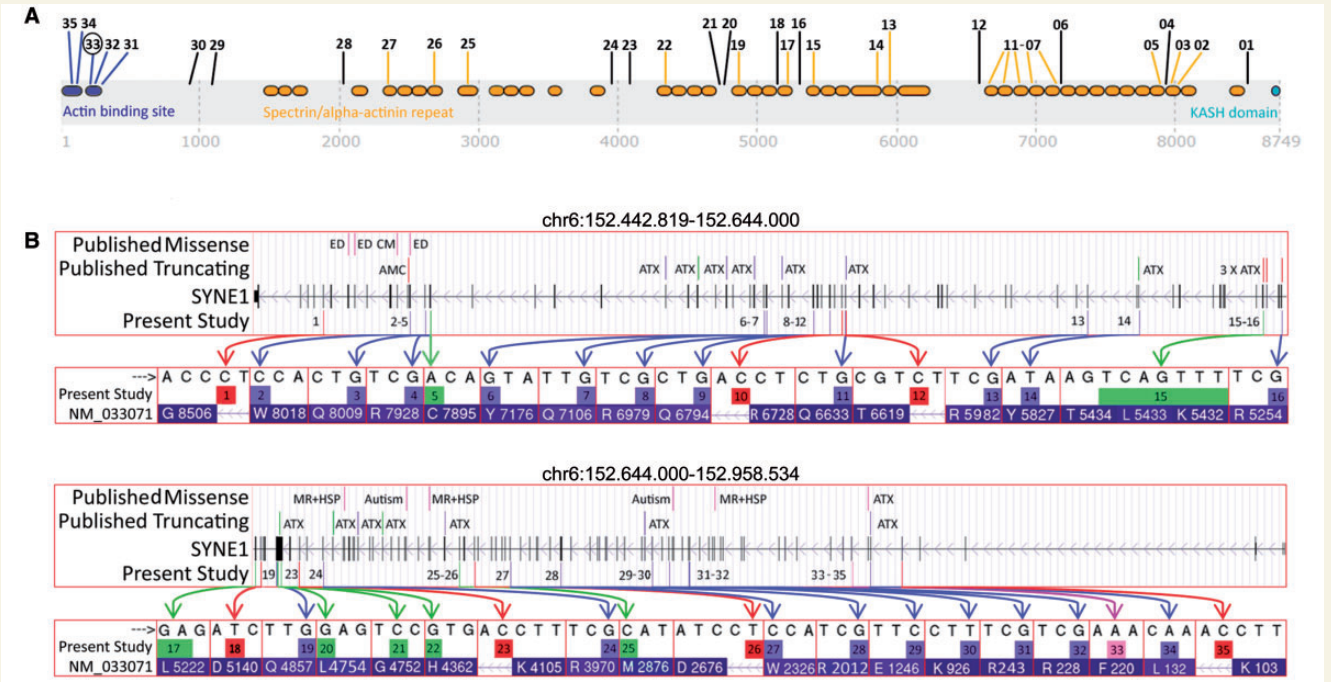

Figure 1 ***SYNE1* mutations.** (**A**) Graphical overview of the mutations found in this study in relation to the SYNE1 domains. Numbers indicate the mutation IDs of the mutations identified in this study (Table 1). Their position indicates the position of the respective mutations in the *SYNE1* gene. Blue = N-terminal actin binding domain [calponin homology domains containing actin binding sites (IPR001715)] and mutations affecting this domain; orange = spectrin/alpha-actinin repeat domains (IPR018159) and mutations affecting these domains; turquoise = KASH domain (C-terminal klarsicht domain) (IPR012315); black = mutations not affecting any of these domains. Mutation 33 (black circle) is the only missense mutation in the present study. (**B**) Overview of the variant types and their location of all published and novel *SYNE1* mutations. The presentation of the giant *SYNE1* gene is split in a first part (chr6:152.442.819–152.644.000; *top*) and a second part (chr6:152.644.000–152.958.534; *bottom*). It presents the variant types of all *SYNE1* mutations found in the present study (*bottom row* of each panel) and other studies (Human Gene Mutation Database) (*top row* of each panel), their location and their annotation with the associated clinical phenotypes. ATX = ataxia; AMC = arthrogryposis multiplex congenita; ED = Emery-Dreifuss muscular dystrophy; CM = cardiomyopathy; MR = mental retardation; HSP = hereditary spastic paraplegia. Note that, except for ATX and AMC, all other phenotypes have been associated only with missense mutations, not truncating mutations in *SYNE1*. Green coloured arrows and boxes = indel mutations; blue coloured arrows and boxes = stop mutations; red coloured arrows and boxes = splice site mutations; purple coloured arrow and box = missense mutation. HG19 genome build. Transcript: NM_033071 > NP_149062.

Pathogenicity of selected base exchanges

Cryptic splice mutation

While six of seven splice mutations affected constitutive splice sites (Table 1), the base exchange c.15419A > G (mutation 18, Family 7)—which appeared as a p.D5140G missense change on the genomic level—was predicted by *in silico* analysis (NNSplice; Reese *et al.*, 1997) to act as a cryptic exonic splice mutation. Specifically, it was predicted to create a new donor site 26 bp upstream of the constitutive 5′ donor splice site of intron 80. To confirm this prediction, we performed reverse transcription and sequencing of *SYNE1* mRNA, revealing a heterozygous deletion of the last 26 nucleotides of exon 80 (r.15419_15444del26) (Fig. 2A), which would result in a protein truncated at residue 5140 (p.D5140Gfs1*). This variant occurred *in trans* with the frameshift duplication/stop gain mutation p.C7895*.

Missense mutation

The missense variant c.659T > C, p.F220S (observed in Family 20): (i) segregated *in trans* with the nonsense variant c.2776A > T, p.K926*; (ii) was absent in all public databases described above; (iii) predicted to be damaging by three of three *in silico* algorithms [MutationTaster (Schwarz *et al.*, 2010; Wang *et al.*, 2010); SIFT (Sim *et al.*, 2012), and PolyPhen-2 (Adzhubei *et al.*, 2010)]; (iv) ranked among the top 1% of all 8.6 billion single nucleotide variants in the GRCh37/hg19 (CADD score: 28.8) (Kircher *et al.*, 2014); and (v) located at a highly conserved position in the actin-binding domain of SYNE1 (Supplementary material). This domain is conserved even in non-metazoan species (paralogues in ichthyospora, fungi and slime mould, E-values in the range of 5×10^{-40} to 10^{-50}), whereas the spectrin domains of SYNE1 provide no significant alignment with paralogues of the same non-metazoan species (E-values > 10). The p.F220S mutation affects one of the six invariant amino

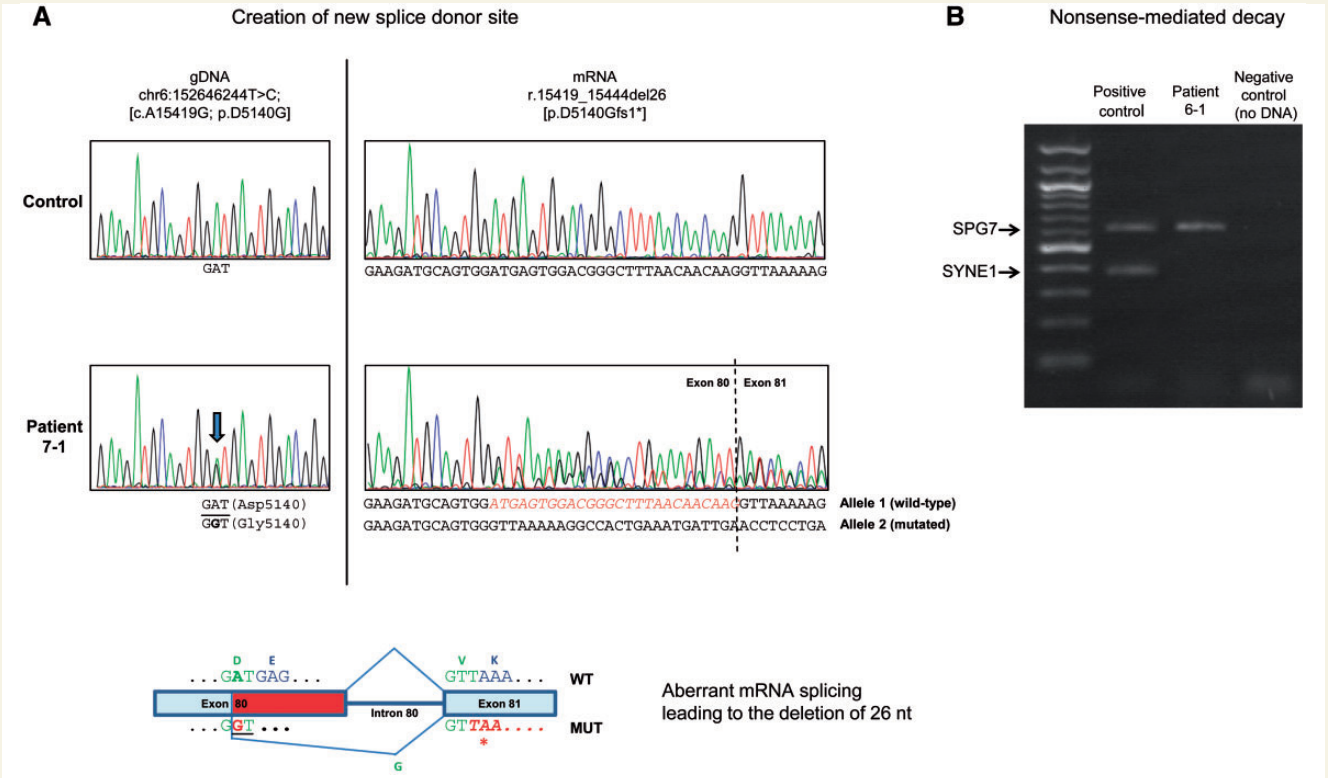

Figure 2 Exemplary mechanisms of *SYNE1* mutations. (**A**) An exonic base exchange leads to activation of a cryptic splice site. (**A**) *SYNE1* transcript analysis reveals that the c.15419A > G (p.D5140G) mutation (identified in Patient 7-1) creates a new splice donor site within exon 80 (GT, underlined in *bottom* panel) resulting in a 26-bp deletion (p.D5140Gfs1*). *Top left*: Sequence analysis of PCR products of amplified genomic DNA showing the A-to-G variant (minus strand) that changes codon 5140 from GAT (Asp) to GGT (Gly). *Top right*: Sequence analysis of amplification products following reverse transcriptase-PCR of *SYNE1* transcript (exons 78–82) from patient's cells showing the presence of the 26-nt deletion (r.15419_15444del26). *Bottom*: Schematic diagram showing the aberrant splicing mechanism which leads to the premature truncation of the protein through the deletion of 26 nucleotides in exon 80 (in red). Premature TAA termination codon in exon 81 is shown in bold red italics. (**B**) Truncating *SYNE1* mutations can lead to nonsense-mediated decay of *SYNE1* mRNA. *SYNE1* mRNA carrying the p.L132* and the p.G4752Efs*10 null mutations undergoes nonsense-mediated decay. PCR amplification from retro-transcribed mRNA was carried out with primers specific for *SYNE1* (exons 4–9) and *SPG7* (exons 6–10) transcripts. Note the complete absence of the *SYNE1* mutant transcript in Patient 6-1 as compared to the control.

acid positions of the second calponin-homology domain in nesprin, spectrin and alpha-actinin homologues (Supplementary material). The biallelic truncating and the missense *SYNE1* variants were also found in the affected sibling of the index patient in Family 20, indicating segregation with disease.

Burden analysis for missense variants in SYNE1

Rare missense *SYNE1* variants were observed in 14/192 alleles (7.3%) from ataxia cases and in 28/500 alleles (5.6%) from disease controls (early-onset Alzheimer dementia) (Supplementary material). Also missense variants in the N-terminal actin-binding domain of *SYNE1* (codon 1–289) were not more frequent in ataxia cases than in controls (Supplementary material). This finding suggests that rare missense *SYNE1* variants seem to present a ubiquitous finding unrelated to specific disease conditions or phenotypes.

In general, these results from the cryptic splice and the missense mutation as well as from the missense variant burden analysis indicate that careful interpretation of single *SYNE1* nucleotide variants is necessary to evaluate possible effects detrimental to SYNE1 function. Such a critical one-by-one debate of *SYNE1* single nucleotide variants is of particular relevance in the future, given the large size of *SYNE1* with its substantial variability.

Absence of *SYNE1* transcript adds support for a loss-of-function mechanism

Truncation of proteins can lead to either toxic gain of function (exerted by the residual protein) or to loss-of-function. To exemplarily investigate the mechanism of action for truncating *SYNE1* mutations, we investigated the pathomechanism of the changes p.L132* and p.G4752Efs*10

(observed in Family 6). No *SYNE1* transcript was amplified by reverse transcriptase-polymerase chain reaction in patient's cells (Fig. 2B), suggesting that both the early nonsense mutation p.L132* and the later frameshift mutation p.G4752Efs*10 cause nonsense-mediated decay of mutant mRNA. The absence of the transcript adds support for a loss-of-function mechanism underlying the detrimental effect of truncating SYNE1 mutations in human SYNE1 disease, as hypothesized earlier (Gros-Louis *et al.*, 2007; Attali *et al.*, 2009).

Severely reduced to absent SYNE1 staining in muscle tissue

Muscle biopsy [available for three different SYNE1 index patients (Patients 13-1, 10-1 and 6-1) originating from three different countries] showed neurogenic changes in all patients, thus corresponding to the clinical/EMG finding of frequent lower motor damage in SYNE1 disease (see below). Upon routine light microscopy and also immunohistochemistry with relevant antibodies, the nuclei had a normal peripheral distribution in the three patients comparable to the control individual (Fig. 3). More precisely, no myopathic and in particular no dystrophic muscle features were seen in any of the three patients, thus contrasting previous findings on dystrophic changes in patients with Emery-Dreifuss muscular dystrophy type 4 (EDMD4; MIM 612998) that were reported in association with heterozygous 'dominant' *SYNE1* (and *SYNE2*) mutations (Zhang *et al.*, 2007*a*).

In line with the suggested loss of protein in SYNE1 patients with truncating mutations, staining of SYNE1 was severely reduced in two patients and absent in one patient (Fig. 3). To control for the possibility that this lack of SYNE1 staining might be an unspecific result or artefact in the SYNE1 samples, control stainings were performed. Control immunolabelling showed normal results for emerin at the inner nuclear membrane and of lamin A/C also in the SYNE1 muscle samples (Fig. 3). No mislocalization of emerin or lamin A/C was seen, thus contrasting previous findings of a mislocalization of these proteins reported in patients with heterozygous *SYNE1* mutations (Zhang *et al.*, 2007*a*).

A broad range of additional non-cerebellar features, including severe and complex early-onset syndromes

We aggregated clinical data from 26 affected subjects belonging to 23 families (median age of disease onset: 22 years, range: 6–40 years; last examination in each individual performed after a median of 25 years of disease duration). Disease started with gait coordination disturbances in 24/26 subjects; in two subjects it began with focal upper limb dystonia (writer's cramp) (Patient 20-1) and lower limb weakness (Patient 23-1), respectively. Five of 26 patients (19%) showed the classical *SYNE1* phenotype of pure cerebellar ataxia that was mildly progressive and started in adulthood (range: 19–36 years) (pure cerebellar ataxia). However, the large majority of patients (21/26, 81%) exhibited at least one additional complicating feature from a large range of non-cerebellar features, both in neurological and non-neurological domains (cerebellar ataxia plus) (Table 2 and Fig. 4A and B).

The most frequent complicating finding was motor neuron dysfunction, observed in 15/26 (58%) of the total cohort (Fig. 4A). This comprised a combination of upper motor neuron dysfunction (bilateral positive extensor plantar reflex and/or spasticity) and lower motor neuron dysfunction (muscle atrophy combined with reduced reflexes; fasciculations clinically or on EMG; or chronic and/or acute neurogenic changes on EMG) in 5/26 patients (19%), only upper motor dysfunction in 8/26 patients (31%), and only lower mutation in 2/26 (8%) patients. Other frequent complicating features across the cohort included: scoliosis (5/26, 19%), sometimes combined with kyphosis, indicative of skeletal abnormalities in SYNE1; slowing of saccades (4/26, 15%), indicative of brainstem dysfunction in SYNE1; and reduced vibration sense of the lower limbs (3/26, 12%), indicative of peripheral nerve and/or dorsal column dysfunction in SYNE1 (for a relative frequency of all main features, see Fig. 4A). A broad range of non-cerebellar oculomotor deficits was seen in single patients across the cohort: square wave jerks, ophthalmoparesis, and strabism including esotropia (Table 2 and Fig. 4A). One patient exhibited mild macroglossia in addition to esotropia, that could not be related to any other disease other than SYNE1 (for image see Supplementary material).

Three cerebellar ataxia plus patients (3/26, 12%; Patients 13-1, 13-2 and 23-1; no consanguinity in either of the two families) showed a particularly severe and complex multisystemic phenotype, comprising very early onset (6–10 years of age) ataxia, spasticity, weakness and muscle wasting of all four limbs, mental retardation (IQ 49–60), dysphagia, pes cavus, and a broad range of variable skeletal and soft-tissue abnormalities such as sacral cysts, pseudarthrosis clavicula, hyperlaxity of joints, achilles tendon contractures, kyphosis, scoliosis, cataract, hypertelorism. All three developed respiratory dysfunction in late adolescence, necessitating BiPAP (bi-level positive airway pressure) ventilation in two of three subjects and leading to premature death at age 36 years in one of them. No obvious second hit in any other disease gene was detected in these patients (Supplementary material). Thus, the complex phenotype in these three subjects does not seem to be explained by a second hit in another gene or to present a qualitatively different condition; rather it seems to illustrate one end on the continuous spectrum of SYNE1 disease, which literally encompasses all of the aforementioned SYNE1-associated domains and includes also mental retardation and respiratory distress (Fig. 4C).

One of the three subjects also showed developmental abnormalities of the visceral organs, such as malrotation

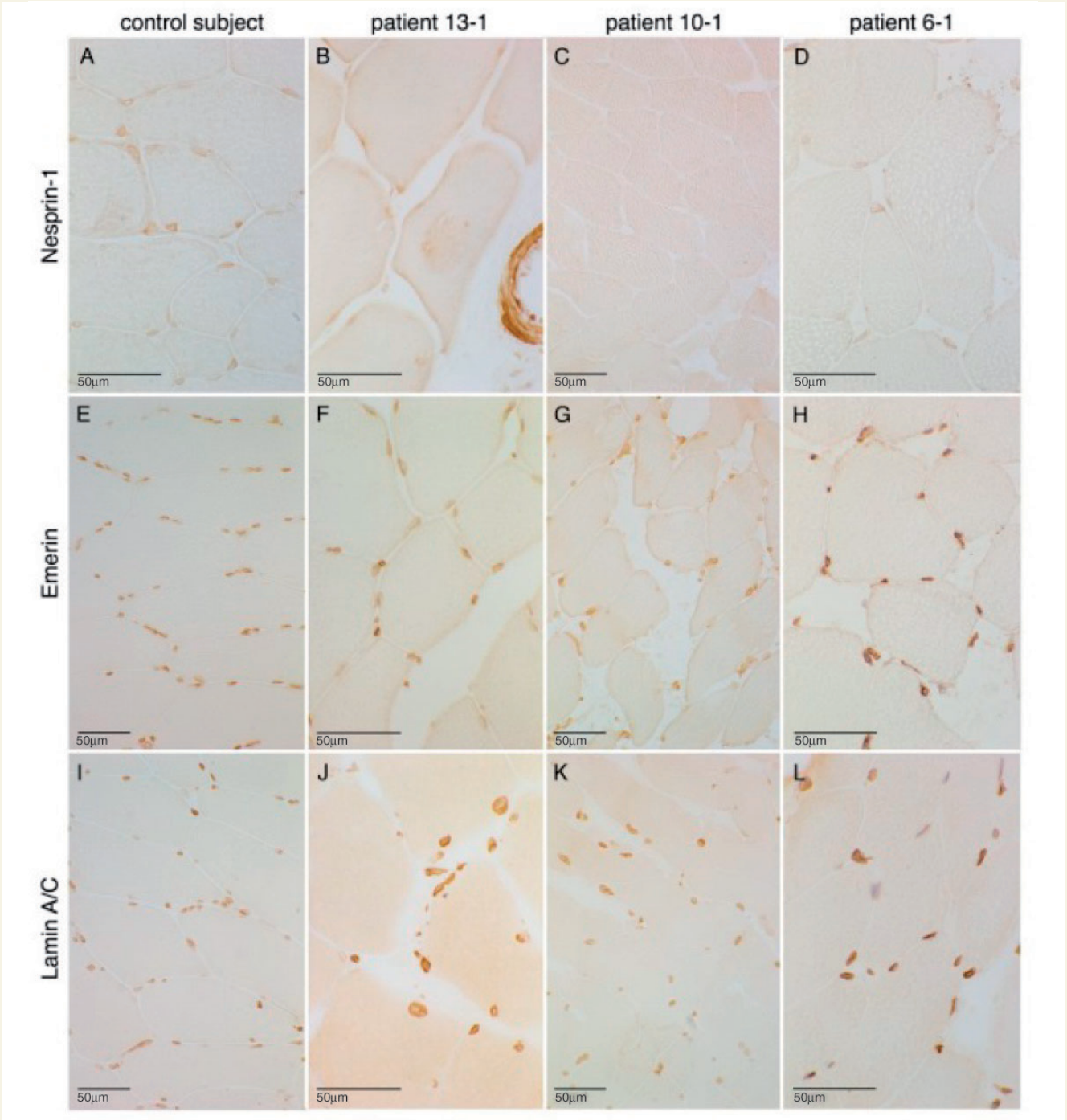

Figure 3 Severely reduced to absent SYNE1 staining in muscle tissue of *SYNE1* patients. Immunohistological findings in control tissue (**A**, **E** and **I**), as well as in the quadriceps muscle biopsies of three different *SYNE1* patients from three different countries: Patient 13-1, Belgian (**B**, **F** and **J**); Patient 10-1, German (**C**, **G** and **K**); and Patient 6-1, Italian (**D**, **H** and **L**). All three patients show a severely reduced to absent staining of the nuclear envelope after immunolabelling of nesprin-1 (**B**–**D**), whereas staining was normal in the control (**A**) (peroxidase-anti-peroxidase technique). To control for an unspecific lack of staining in the SYNE1 patients, further control stainings were performed. Immunolabelling of emerin and lamin A/C at the inner nuclear membrane was normal in all three patients as well as the control (**E**–**H** and **I**–**L**, respectively) (avidin-biotin complex technique).

of the colon and unilateral positioning of both kidneys at right pelvis. However, future studies in SYNE1 patients are warranted to confirm whether such visceral features are indeed part of its phenotypic spectrum.

Electrophysiological findings

Motor evoked potentials, available for eight patients, were prolonged or not evoked in six of eight patients (75%), all

Table 2 Clinical, imaging and electrophysiological features of SYNE1 patients

Patient ID (family-individual)	Phenotype category	Genotype (cDNA)	Origin/ gender	Age of onset	Age at last examination (years)	SARA score	Cerebellar ataxia	Dysfunction upper motor neuron	Dysfunction lower motor neuron	Additional clinical features	Cerebellar atrophy (MRI)	Peripheral neuropathy (NCS)	EMG changes (muscle)	Abnormal MEPS
1-1	Pure CA	c.13086delC; c.13086delC	Turkish/m	22	32	13	+	-	-	-	+	-	-	n.d.
3-1	Pure CA	c.15760C>T; c.15760C>T	Turkish/f	25	40	12	+	-	-	-	+	-	n.d.	n.d.
7-1	Pure CA	c.23684_23685insACGCC TGTGCCACTGATGCCGAGTG; c.15419A>G	Italian/f	36	48	5	+	-	-	-	+	-	-	-
16-1	Pure CA	c.6978G>A; c.6978G>A	French/f	27	62	18	+	-	-	-	+	-	-	n.d.
18-1	Pure CA	c.24054G>A; c.16294_16300delA AACTGA	German/f	19	23	9	+	-	-	-	+	-	-	n.d.
4-1	CA plus	c.24025C>T; c.15665_15666delTC	German/f	40	67	18	+	Signs +; spasticity LL	-	Urge incontinence	+	-	n.d.	Abnormal LL
5-1	CA plus	c.23782C>T; c.8627_8628insAT	Italian/m	35	75	25	+	-	+	Slow saccades	+	n.d.	n.d.	n.d.
9-1	CA plus	c.21316C>T; c.11908C>T	German/m	28	46	15,5	+	Signs +; spastic gait	-	Mild macroglossia; esotropia;	+	n.d.	n.d.	n.d.
10-1	CA plus	c.19855-1G>C; c.19855-1G>C	German/f	21	39	22	+	Signs +; spasticity LL and UL	-	Urge incontinence	+	-	-	Abnormal UL + LL
11-1	CA plus	c.19897C>T; c.19897C>T	Turkish/f	18	25	16,5	+	Signs +	+	Strabism divergens, fasciculation face, fibrillation tongue, reduced vibration sense, depression, CK elevation	+	-	Chronic neurogenic	Abnormal UL + LL
12-1	CA plus	c.21528C>A; c.20935C>T	Belgian/f	6	36	33	+	Signs +; spasticity LL and UL	+	Respiratory distress, mental retardation, sacral cyst, malrotation colon, pseudarthrosis clavicula, 2 kidneys right sided, kyphosis, scoliosis, CK elevation, pes cavus, strabism, cataract, myoclonus	+	-	Acute neurogenic	Abnormal LL
12-2	CA plus	c.21528C>A; c.20935C>T	Belgian/m	6	28	33	+	Signs +; spasticity LL	+	Respiratory distress (BIPAP all day), mental retardation (IQ = 60), hypertelorism, CK elevation, pes cavus, hyperlaxity, achilles tendon contractures	+	-	Acute + chronic neurogenic	n.d.
13-1	CA plus	c.682C>T; c.682C>T	Moroccan/f	30	42	14	+	Signs +; spasticity LL;	-	-	+	-	n.d.	n.d.
13-2	CA plus	c.682C>T; c.682C>T	Moroccan/f	28	40	14	+	Signs +; spastic gait	-	-	+	-	-	n.d.
14-1	CA plus	c.20380C>T; c.17480dup	German/m	15	29	8	+	Signs +; spasticity LL	+	Pes cavus	+	-	n.d.	Abnormal UL + LL
19-1	CA plus	c.17944C>T; c.17944C>T	Italian/f	10	49	28	+	Signs +; spasticity LL	-	Slow saccade initiation, horizontal ophtalmoparesis, facial myokymia	+	n.d.	n.d.	n.d.
20-1	CA plus	c.2776A>T; c.659T>C	French/f	24	70	24	+	-	+; proximal	Reduced vibration sense, urge incontinence, bulging eyes, upper limb dystonia	+	n.d.	n.d.	n.d.
21-1	CA plus	c.14261dup; c.6034C>T	Italian/f	16	50	20	+	Signs +	-	Urge incontinence	+	n.d.	n.d.	n.d.
22-1	CA plus	c.727C>T; c.727C>T	Italian/m	20	65	18	+	Signs +	-	Scoliosis, dysphagia	+	+; mild sensory axonal, LL	-	-
23-1	CA plus	c.23782C>T; c.G20183 + 1G>C	Italian/m	10	21	22	+	Signs +; spastic gait	+	Cognitive deficit (IQ = 49), slow saccades, CK elevation, restrictive ventilatory defect, pes cavus	+	+, motor axonal	Chronic neurogenic	Abnormal UL + LL

(continued)

Table 2 Continued

Patient ID (family-individual)	Phenotype category	Genotype (cDNA)	Origin/ gender	Age of onset	Age at last examination (years)	SARA score	Cerebellar ataxia	Dysfunction upper motor neuron	Dysfunction lower motor neuron	Additional clinical features	Cerebellar atrophy (MRI)	Peripheral neuropathy (NCS)	EMG changes (muscle)	Abnormal MEPS
2-1	CA plus	c.14569C>T; c.309 + 1G>A	German/m	24	63	14	+	-	-	Slow vertical saccades	+	-	n.d.	n.d.
6-1	CA plus	c.14255delG; c.395T>A	Italian/f	20	27	13	+	-	-	Scoliosis	+	-	-	n.d
8-1	CA plus	c.25516-1G>A; c.8026-2A>G	Italian/fi	25	65	22	+	-	-	Scoliosis; kyphosis	+	-	-	n.d.
15-1	CA plus	c.12315 + 1G>A; c.12315 + 1G>A	French/m	27	43	13	+	-	-	Square wave jerks, horizontal ophtalmoparesis, mild microretrognathism, unilateral ptosis	n.d.	n.d.	n.d.	n.d.
15-2	CA plus	c.12315 + 1G>A; c.12315 + 1G>A	French/f	17	58	11	+	-	-	Scoliosis, seizures at age 2 year, square wave jerks	n.d.	n.d.	n.d.	n.d.
17-1	CA plus	c.3736G>T; c.3736G>T;	Algerian/f	7	32	21	+	-	-	Pes cavus	+	-	-	n.d.

Patient ID = family number-individual number; m = male; f = female; pure CA= pure cerebellar ataxia; CA plus = cerebellar ataxia plus at least one additional system damage; + = present; - = absent; CK = creatine kinase; SARA = scale for the assessment and rating of ataxia; upper motor neuron signs = extensor plantar response positive and/or hyperreflexia of muscle tendon reflexes; UL = upper limb, LL = lower limb; NCS = nerve conduction studies; n.d. = not done.

of them showing also clinical signs of upper motor neuron damage (Table 2). Nerve conduction studies, available for 19 patients, were normal in 17/19 patients (89%), while one patient showed a peripheral motor neuropathy and one patient a mild sensory axonal neuropathy, demonstrating that peripheral neuropathy is a rather infrequent feature in SYNE1 disease.

Imaging findings

Cerebral MRI, available from 24 patients, consistently showed marked cerebellar atrophy in all 24/24 (100%) patients (for exemplary illustration, see Fig. 5). ^{18}F-FDG-PET imaging performed in two exemplary subjects with ataxia-motor neuron disease revealed a marked homogenous ^{18}F-FDG decrease in both cerebellar hemispheres in both subjects and, on visual inspection, also of the pontine brainstem, which reached statistical significance in Patient 10-1 with a Z-score of 3 and a trend in Patient 9-1 with a Z-score of 1.5 (semiquantitative PET, normalization to global mean activity and comparison to an age-adjusted database) (Fig. 5). These imaging findings provide proof-of-concept functional imaging evidence that dysfunctions in SYNE1 patients extend beyond the cerebellar domain to include in particular the pons, thus complementing our clinical findings of extra-cerebellar features in SYNE1.

Discussion

SYNE1: a recurrent recessive ataxia worldwide, with mutations spanning across the entire gene

So far, autosomal-recessive cerebellar ataxia (ARCA) due to *SYNE1* mutations has been described mainly in Quebec, Canada, with few families having been identified outside French-Canadian populations (Izumi *et al.*, 2013; Noreau *et al.*, 2013). Reporting by far the largest series of *SYNE1* patients outside Quebec, we here show that SYNE1 deficiency is in fact a relatively common cause of recessive ataxia worldwide, yielding an estimated frequency of at least 5.3% after exclusion of Friedreich's ataxia and the most common repeat expansion SCAs. This is probably a rather conservative estimate, given the fact that our approach used only a very preliminary NGS-based approach to screen for copy number variants (CNVs) and that it was very restrictive on including missense variants. Future studies might be able to identify damaging CNVs in the large *SYNE1* gene, which would further increase the relative frequency of subjects with truncating *SYNE1* mutations.

Our genetic findings more than double the number of truncating *SYNE1* mutations identified so far: while <15 different truncating *SYNE1* mutations have been described, we here identified 33 novel truncating (plus one novel missense) *SYNE1* mutations, which are scattered throughout

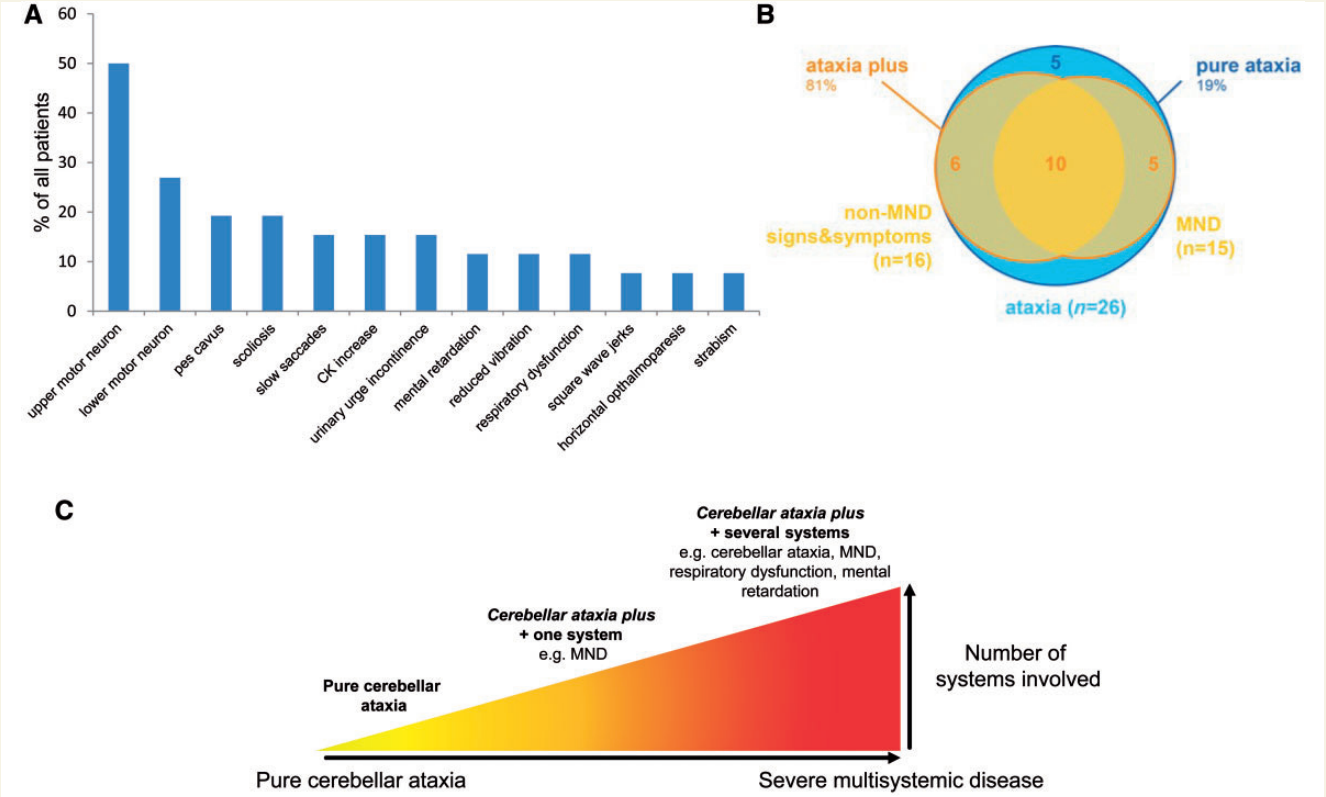

Figure 4 The phenotypic spectrum of SYNE1 disease. (**A**) Frequency of non-cerebellar features in SYNE1. Relative frequencies of non-cerebellar features observed in the $n = 26$ SYNE1 patients investigated in this study. Note that several patients showed $\geqslant 2$ non-cerebellar disease features. (**B**) The relative share of main SYNE1 phenotypes. This figure illustrates that only a minor share of SYNE1 patients shows pure cerebellar ataxia (blue), whereas the large majority show cerebellar ataxia plus phenotypes (yellow), in particular cerebellar ataxia plus motor neuron disease (MND). The latter combination is thereby not a distinct ataxia plus-phenotype, but is commonly associated also with other non-motor neuron disease signs (see overlap group comprising of $n = 10$ subjects). (**C**) The continuous spectrum of SYNE1 disease. The clinical spectrum of neurological and non-neurological *SYNE1* features presented in **A** unfolds along a continuous spectrum of disease. Variable combinations of these features can be found in different SYNE1 patients reaching from pure cerebellar ataxia (*left*) via cerebellar ataxia plus damage of one or two additional systems [e.g. motor neuron disease (MND)] to cerebellar ataxia as part of severe multisystemic neurodegenerative syndrome (*right*). In addition to ataxia and motor neuron disease, the latter can include also mental retardation, respiratory distress and visceral organs. The phenotype of mild, slowly progressive pure cerebellar ataxia, which has been considered the most prominent phenotype of SYNE1 so far (Gros-Louis *et al.*, 2007; Noreau *et al.*, 2013), thus represents only one far edge of this broad disease spectrum. CK = creatine kinase.

all parts of this gigantic gene. Almost all mutations are private, identified in single families without obvious mutational hot spot regions. Five mutations affected the coding sequence of the SYNE1 isoform Nesprin 1α (see mutations 1–5, Table 1). As no mutations linked to ataxia had been previously found in this domain (Razafsky and Hodzic, 2015), it was suggested that a protein encoded by these exons may underlie a distinct pathology in humans (Razafsky and Hodzic, 2015). However, here we show that mutations in this sequence can lead to the same phenotypic features as mutations in other parts of *SYNE1*.

Taken together, these findings have also major implications for future clinic-genetic testing strategies in unresolved ARCA patients around the world: they demonstrate that also in non-Canadian populations current genetic testing approaches have to include the large *SYNE1* gene by using approaches that tightly capture all of its exons.

SYNE1 spectrum: from late-onset pure cerebellar ataxia to complex neuromuscular disease with mental retardation

Recessive ataxia due to *SYNE1* mutations is commonly perceived to present as a slowly progressive, relatively pure cerebellar ataxia with only mild and infrequent extra-cerebellar symptoms (e.g. brisk reflexes in 33%; Dupre *et al.*, 2007), starting in adult age (Dupre *et al.*, 1993/2012; Gros-Louis *et al.*, 2007; Noreau *et al.*, 2013; Fogel *et al.*, 2014). However, here we show that pure cerebellar ataxia represents rather a relatively infrequent phenotypic cluster along a broad multidimensional SYNE1-associated spectrum of neurodegenerative disorders. With 81% of all patients exhibiting variable additional non-cerebellar features both in neurological and

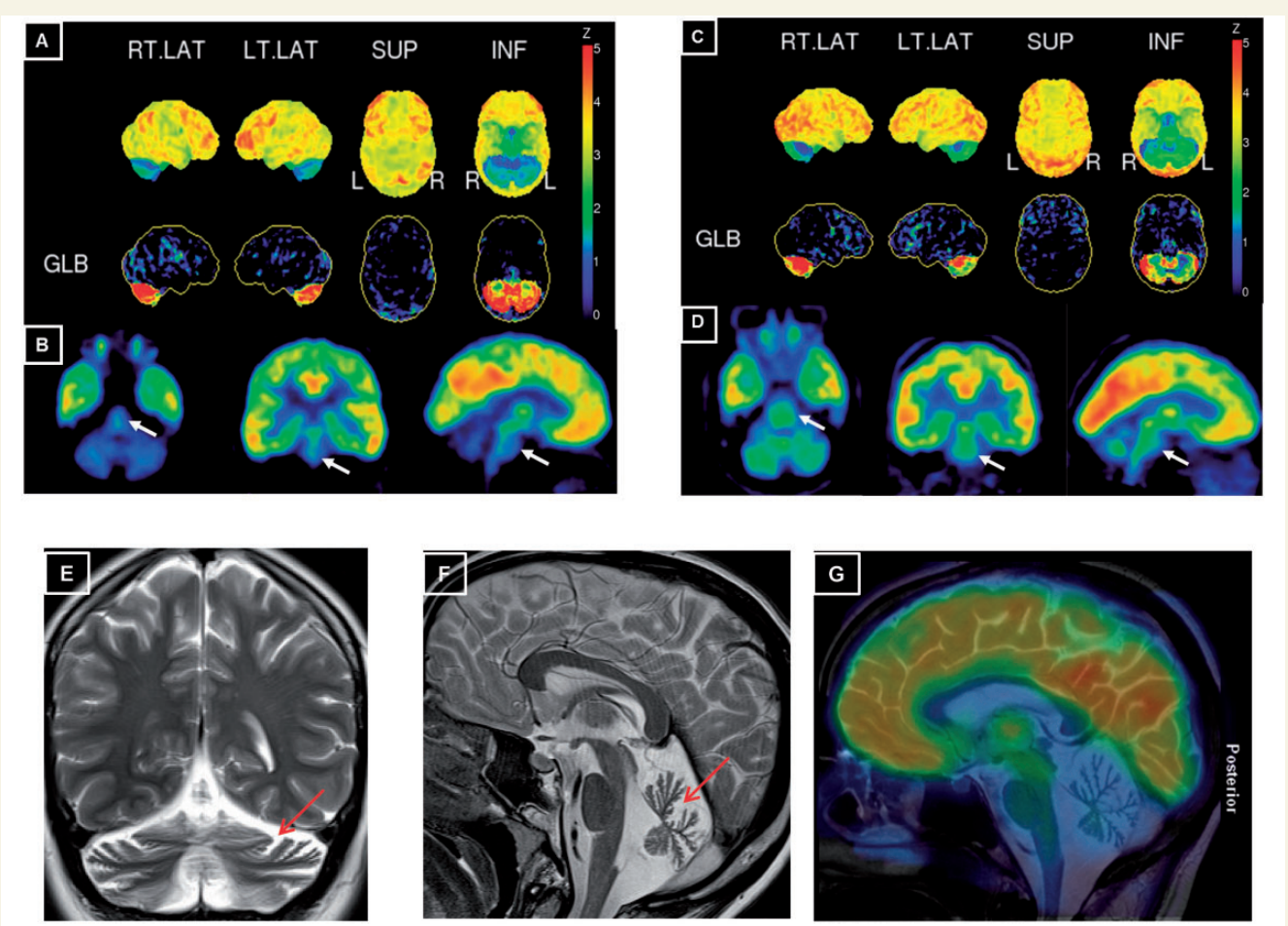

Figure 5 Cerebral ^{18}F- FDG PET and MRI in exemplary SYNE1 patients. (**A** and **C**) Surface projections of the ^{18}F-FDG PET scans of Patient 10-1 at age 37 years (**A**) and Patient 9-1 at age 45 years (**C**). The upper rows in **A** and **C** show the surface projection map of cerebral glucose metabolism normalized to the maximum of the acquisition. The lower rows show the deviation of an age-adjusted normal database after normalization to a global mean calculation (GLB) of metabolic activity. On both projections, a marked homogenous bilateral reduction of cerebellar FDG metabolism can be seen in both subjects. (**B** and **D**) Tomographic projections after automated fitting. For both Patient 10-1 (**B**) and Patient 9-1 (**D**) a reduction of FDG-metabolism is also clearly visible in the brainstem (white arrows), which reached statistical significance in Patient 10 with a Z-score of 3 and a trend in Patient 9-1 with a Z-score of 1.5 (semiquantitative PET, deviation after normalization to the global mean). (**E** and **F**) T_2-weighted MRI scans in Patient 18-1 at age 21 years shows marked vermian atrophy (**F**) and cortical hemisphere atrophy (**E**) of the cerebellum (red arrows). (**G**) Fusion image of ^{18}F-FDG PET scan of Patient 10-1 onto a central paramedian sagittal T_2-weighted MRI scan shows considerable hypometabolism in the cerebellum and in the pons, whereas FDG metabolism is normal in the cortical cerebral regions.

non-neurological domains, a multisystemic phenotype seems to be the rule rather than the exception in SYNE1 disease. Apart from cerebellar ataxia, this spectrum includes upper motor neuron disease, lower motor neuron disease, brainstem dysfunction (e.g. saccadic slowing), and a variable range of musculoskeletal abnormalities (e.g. kyphosis, scoliosis, pes cavus, contractures). Variable combinations of these features can be found in different SYNE1 patients along a continuous spectrum of disease. This spectrum ranges from (i) pure cerebellar ataxia; via (ii) cerebellar ataxia plus damage of one or two additional systems (such as motor neuron disease, thus giving rise to spastic ataxia and complicated hereditary spastic paraplegia phenotypes); to (iii) cerebellar ataxia as part of severe multisystemic neurodegenerative syndromes. The latter encompass literally all of the aforementioned SYNE1-associated domains and include also mental retardation, respiratory distress and possibly visceral organ involvement (Table 2; for graphic illustration of the SYNE1 disease continuum, see Fig. 4B and C).

The complex early-onset neurodegenerative syndrome does not seem to present a mere coincidental finding (that might be unrelated to the *SYNE1* mutations), but rather reflects a phenotypic cluster systematically related to *SYNE1* mutations. This is indicated by the fact that we identified three patients from two different families with this severe phenotypic combination. In fact, a fourth patient with early-onset complex *SYNE1* ataxia-motor neuron disease and respiratory dysfunction has recently been described as a single case in a Japanese family (Izumi *et al.*, 2013),

thus increasing the evidence to three different families. We now show that this phenotypic cluster is not a qualitatively distinct syndrome, but rather a combination of *SYNE1*-associated features that can each be found in isolation or as part of less complex phenotypic clusters in other *SYNE1* patients along a continuous spectrum of disease. Although we did not find obvious mutation–phenotype correlations, different *SYNE1* mutations might differentially affect the multiple SYNE1 splicing isoforms which vary greatly in size and tissue-specific expression patterns (Zhang *et al.*, 2010; Razafsky and Hodzic, 2015), thus possibly explaining parts of the phenotypic variability observed here. In fact, *SYNE1* mutant mice show variable phenotypes depending on the splicing isoform that was targeted (for overview see Zhang *et al.*, 2010).

Our findings have important implications for clinico-genetic counselling. They revise current clinical notions about the benign disease course of *SYNE1*-disease, including the notion that life expectancy was normal (Dupre *et al.*, 1993/2012; Gros-Louis *et al.*, 2007). They show that, at least in some patients, *SYNE1*-disease can start already as a developmental disease with mental retardation and early-onset ataxia in the first decade of life, and that it can lead to premature death due to respiratory dysfunction in the mid-adult age (age 30–40 years).

Bridging the gap between SYNE1 ataxia and arthrogryposis syndromes

Truncating recessive *SYNE1* mutations have been described as a cause of an arthrogryposis multiplex congenita syndrome in a single Palestinian family presenting with infantile-onset hypotonia, bilateral club foot, progressive motor decline in the first decade, scoliosis and restrictive lung disease, yet without ataxia or motor neuron disease (Attali *et al.*, 2009) (for location of these mutations, see Fig. 1B). This musculoskeletal infantile-onset phenotypic cluster was proposed as a 'distinct human disease phenotype' of SYNE1, separate from the neurological phenotype (Attali *et al.*, 2009). As several of our ataxic SYNE1 patients, however, also show scoliosis/kyphosis, restrictive lung disease, foot deformities, and other neuromuscular abnormalities as part of their early-onset multisystemic disease, and also carry truncating mutations in the same or neighbouring gene region (Fig. 1B), we here suggest that such arthrogryposis syndromes do not represent qualitatively distinct phenotypes, but rather clusters of variably combined neurologic and non-neurological features along the continuum of SYNE1 disease.

It remains more questionable whether this SYNE1 disease continuum also includes the dominant form EDMD4 (Zhang *et al.*, 2007*a*). Although a phenotypic overlap might be theoretically conceivable, as indicated by our clinical findings, this syndrome has been linked only to heterozygous missense mutations in *SYNE1* (Zhang *et al.*, 2007*a*) (Fig. 1B), but not to biallelic truncating mutations. As advanced genomic techniques now allow us to appreciate the immense variability of the *SYNE1* gene and to determine the frequency of rare *SYNE1* missense variants in controls (e.g. 28/500 = 5.6% rare missense alleles in our control dataset with early-onset Alzheimer dementia; Supplementary material), the pathogenicity of such variants previously related to EDMD4 needs to be critically evaluated against current standards. Furthermore, findings on muscle biopsies between subjects with EDMD4 and the here reported cases with biallelic truncating mutations differ substantially; while EDMD4 subjects showed dystrophic myopathic changes and in particular mislocalization of emerin or lamin A/C (Zhang *et al.*, 2007*a*), none of these features was seen in the muscle cells of any of our subjects (Fig. 3). Although this might be explained by a different *SYNE1*-related pathomechanism, this patho-morphological discrepancy, in addition to the genetic concerns mentioned above, indicates a possible over-interpretation of heterozygous *SYNE1* variants in the context of EDMD4 and warrants a critical re-evaluation of these historic findings.

A widespread functional role of SYNE1 in various tissues

Our findings on widespread extra-cerebellar dysfunctions in human SYNE1 disease complement and recapitulate some of the key features of SYNE1/Nesprin 1 knock-out mouse models. Key features in mice include kyphoscoliosis, respiratory failure, and shortened survival (Zhang *et al.*, 2007*b*, 2010; Puckelwartz *et al.*, 2009). We now show systematically that these features are also part of the human disease spectrum, thus bridging the cross-species gap.

Moreover, our findings on extra-cerebellar dysfunctions might provide new insights into the pathophysiology underlying SYNE1-associated neurodegeneration. Recent work has shown that a specific SYNE1 isoform devoid of the KASH domain (KLNes1g) is specifically abundant in the cerebellum (in particular in the granule cell layer), where it might be involved in vesicular trafficking and/or in dendritic membranes' structural organization (Razafsky and Hodzic, 2015). Our clinical, electrophysiological and imaging observations of multisystemic damage in *SYNE1* patients, however, indicate that intact SYNE1 transcripts seem to be functionally important not only for cerebellar, but also for motor and brainstem neurons. They thus stimulate future molecular research aiming to identify the specific functional role of SYNE1 in these neuron types. For example, the proposed interaction of *SYNE1* transcripts with vesicular trafficking proteins such as KIF5C, suggested for cerebellar neurons (Razafsky and Hodzic, 2015), might also apply to motor neurons. Aberrant vesicular trafficking dynamics is a common process underlying motor neuron degeneration (as in hereditary spastic paraplegias; Crosby and Proukakis, 2002), and mutations in KIF5C have been

shown to include upper motor neuron damage (Poirier *et al.*, 2013).

In sum, our clinical, electrophysiological and imaging findings suggest a widespread functional role of SYNE1 in many different tissues in humans, which is in line with its ubiquitous expression (Apel *et al.*, 2000; Gros-Louis *et al.*, 2007; Zhang *et al.*, 2010). This ubiquitous expression of SYNE1—and, in turn, its absence in case of protein truncation—might help to find diagnostic biomarkers for the disease. Our results suggest that severely reduced to absent SYNE1 staining in muscle tissue, which was observed in all three available samples, may represent a diagnostic marker that indicates underlying truncating *SYNE1* mutations. If confirmed in larger sample cohorts, SYNE1 staining of muscle tissue might thus become a helpful auxiliary tool in the histochemical work-up of muscle biopsies of future patients with unresolved neurodegenerative and neuromuscular diseases. It is likely that many more SYNE1 patients with both relatively pure ataxia as well as complex neuromuscular phenotypes will be identified worldwide in the very next years.

Acknowledgements

We are grateful to J. Reichbauer (Hertie-Institute for Clinical Brain Research, Tübingen), B. Kootz (Institute of Medical Genetics and Applied Genomics, University of Tübingen), Inge Bats (Antwerpen), L. A. Pacha L, T. Benhassine, M. Tazir (Algiers, Algeria), P. De Liège (Niort, France), Christophe Verny (Anger), N. Drouot (IGBMC, Illkirch Graffenstaden, France), and M. Renaud (Neurology, Hôpitaux Universitaires de Strasbourg, France) for technical support and help in recruiting subjects.

Funding

This study was supported by the Interdisciplinary Center for Clinical Research IZKF Tübingen (grant 2191-0-0 to M.S., grant 1970-0-0 to R.S.), the European Union (grant F5-2012-305121 'NEUROMICS' to L.S. and grant PIOF-GA-2012-326681 'HSP/CMT genetics' and 'NEUROLIPID' (01GM1408B) to R.S.), E-RARE grants of the respective national research ministries to the EUROSCAR project (to L.S., P.B., M.K. and F.T.) (grant 01GM1206), grant RF-2009-1539841 from the Italian Ministry of Health to F.T., the EUROSPA project (grant 01GM0807) (to L.S. and P.B.), and the National Institute of Health (NIH) (grants 5R01NS072248 to S.Z., 1R01NS075764 to S.Z., 5R01NS054132 to S.Z., and 2U54NS065712 to S.Z.).

Conflict of interest

Dr Klopstock has performed consultancies for Actelion Pharmaceuticals Ltd, GenSight Biologics, Gerson Lehrman Group, USA, and FinTech Global Capital, Japan. He has been serving as a Section Editor for BMC Medical Genetics from 2011-2015. Dr Anheim received received honoraria, consulting fees and travel reimbursements from Actelion Pharmaceuticals Ltd, Abbvie, Novartis, Teva and Lundbeck.

All other authors report no disclosures.

Supplementary material

Supplementary material is available at *Brain* online.

References

Adzhubei IA, Schmidt S, Peshkin L, Ramensky VE, Gerasimova A, Bork P, et al. A method and server for predicting damaging missense mutations. Nat Methods 2010; 7: 248–9.

Apel ED, Lewis RM, Grady RM, Sanes JR. Syne-1, a dystrophin- and Klarsicht-related protein associated with synaptic nuclei at the neuromuscular junction. J Biol Chem 2000; 275: 31986–95.

Attali R, Warwar N, Israel A, Gurt I, McNally E, Puckelwartz M, et al. Mutation of SYNE-1, encoding an essential component of the nuclear lamina, is responsible for autosomal recessive arthrogryposis. Hum Mol Genet 2009; 18: 3462–9.

Crosby AH, Proukakis C. Is the transportation highway the right road for hereditary spastic paraplegia? Am J Hum Genet 2002; 71: 1009–16.

Dupre N, Gros-Louis F, Bouchard JP, Noreau A, Rouleau GA. SYNE1-related autosomal recessive cerebellar ataxia. In: Pagon RA, Bird TD, Dolan CR, Stephens K, Adam MP, editors. GeneReviews. Seattle, WA; 1993/2012. p. accessed on July 13th, 2014.

Dupre N, Gros-Louis F, Chrestian N, Verreault S, Brunet D, de Verteuil D, et al. Clinical and genetic study of autosomal recessive cerebellar ataxia type 1. Ann Neurol 2007; 62: 93–8.

Fogel BL, Lee H, Deignan JL, Strom SP, Kantarci S, Wang X, et al. Exome sequencing in the clinical diagnosis of sporadic or familial cerebellar ataxia. JAMA Neurol2014; 71: 1237–46.

Forster S, Vaitl A, Teipel SJ, Yakushev I, Mustafa M, la Fougere C, et al. Functional representation of olfactory impairment in early Alzheimer's disease. J Alzheimers Dis 2010; 22: 581–91.

Gonzalez MA, Lebrigio RF, Van Booven D, Ulloa RH, Powell E, Speziani F, et al. GEnomes Management Application (GEM.app): A New Software Tool for Large-Scale Collaborative Genome Analysis. Hum Mutat 2013; 34: 842–846.

Gonzalez M, Falk MJ, Gai X, Postrel R, Schule R, Zuchner S. Innovative genomic collaboration using the GENESIS (GEM.app) platform. Hum Mutat 2015; 36: 950–956.

Gros-Louis F, Dupre N, Dion P, Fox MA, Laurent S, Verreault S, et al. Mutations in SYNE1 lead to a newly discovered form of autosomal recessive cerebellar ataxia. Nat Genet 2007; 39: 80–5.

Hamza W, Ali Pacha L, Hamadouche T, Muller J, Drouot N, Ferrat F, et al. Molecular and clinical study of a cohort of 110 Algerian patients with autosomal recessive ataxia. BMC Med Genet 2015; 16: 36.

Izumi Y, Miyamoto R, Morino H, Yoshizawa A, Nishinaka K, Udaka F, et al. Cerebellar ataxia with SYNE1 mutation accompanying motor neuron disease. Neurology 2013; 80: 600–1.

Kircher M, Witten DM, Jain P, O'Roak BJ, Cooper GM, Shendure J. A general framework for estimating the relative pathogenicity of human genetic variants. Nat Genet 2014; 46: 310–15.

Martin JJ, Ceuterick C, Van Goethem G. On a dominantly inherited myopathy with tubular aggregates. Neuromuscul Disord 1997; 7: 512–20.

Noreau A, Bourassa CV, Szuto A, Levert A, Dobrzeniecka S, Gauthier J, et al. SYNE1 mutations in autosomal recessive cerebellar ataxia. JAMA Neurol 2013; 70: 1296–31.

Poirier K, Lebrun N, Broix L, Tian G, Saillour Y, Boscheron C, et al. Mutations in TUBG1, DYNC1H1, KIF5C and KIF2A cause malformations of cortical development and microcephaly. Nat Genet 2013; 45: 639–47.

Puckelwartz MJ, Kessler E, Zhang Y, Hodzic D, Randles KN, Morris G, et al. Disruption of nesprin-1 produces an Emery Dreifuss muscular dystrophy-like phenotype in mice. Hum Mol Genet 2009; 18: 607–20.

Razafsky D, Hodzic D. A variant of Nesprin1 giant devoid of KASH domain underlies the molecular etiology of autosomal recessive cerebellar ataxia type I. Neurobiol Dis 2015; 78: 57–67.

Reese MG, Eeckman FH, Kulp D, Haussler D. Improved splice site detection in Genie. J Comput Biol 1997; 4: 311–23.

Schmitz-Hubsch T, du Montcel ST, Baliko L, Berciano J, Boesch S, Depondt C, et al. Scale for the assessment and rating of ataxia: development of a new clinical scale. Neurology 2006; 66: 1717–20.

Schwarz JM, Rodelsperger C, Schuelke M, Seelow D. MutationTaster evaluates disease-causing potential of sequence alterations. Nat Methods 2010; 7: 575–6.

Sim NL, Kumar P, Hu J, Henikoff S, Schneider G, Ng PC. SIFT web server: predicting effects of amino acid substitutions on proteins. Nucleic Acids Res 2012; 40: W452–7.

Wang K, Li M, Hakonarson H. ANNOVAR: functional annotation of genetic variants from high-throughput sequencing data. Nucleic Acids Res 2010; 38: e164.

Zhang J, Felder A, Liu Y, Guo LT, Lange S, Dalton ND, et al. Nesprin 1 is critical for nuclear positioning and anchorage. Hum Mol Genet 2010; 19: 329–41.

Zhang Q, Bethmann C, Worth NF, Davies JD, Wasner C, Feuer A, et al. Nesprin-1 and -2 are involved in the pathogenesis of Emery Dreifuss muscular dystrophy and are critical for nuclear envelope integrity. Hum Mol Genet 2007a; 16: 2816–33.

Zhang X, Xu R, Zhu B, Yang X, Ding X, Duan S, et al. Syne-1 and Syne-2 play crucial roles in myonuclear anchorage and motor neuron innervation. Development 2007b; 134: 901–8.